State Selective Predissociation Spectroscopy of Hydrogen Bromide Ions (HBr^+) via the $^2\Sigma^+ \leftarrow {}^2\Pi_i(i=1/2, 3/2)$ Transition

Martin Penno, Andrea Holzwarth, and Karl-Michael Weitzel*

Institut für Physikalische und Theoretische Chemie, Freie Universität Berlin, Takustrasse 3, 14195 Berlin, Germany

Received: October 6, 1997; In Final Form: January 6, 1998

The photodissociation of hydrogen bromide ions (HBr^+) has been investigated via the $^2\Sigma^+(v'=1, 2, 3,$ and $4) \leftarrow {}^2\Pi_i(i=1/2, 3/2, v''=0)$ transitions. The spectra reveal that state selective photodissociation with complete resolution of the rotational, orbital, and spin angular momentum as well as the parity of the HBr^+ ions is possible in the $^2\Sigma^+(v'=1, 2)$. The analysis of the spectra yields the rotational constants, the spin−rotation coupling constant, and the orbit−rotation coupling constant in the respective electronic states. All angular momentum eigenstates of the $^2\Sigma^+(v'=2)$ state (and of all higher vibrational states) predissociate. The first eigenstate in the $^2\Sigma^+(v'=1)$ state that predissociates is the $J' = 25/2$, $R' = 12$ state. The lifetime of HBr^+ is found to decrease significantly with increasing vibrational excitation in the $^2\Sigma^+$ state. Within the experimental error limits no J dependence of the lifetime is observed.

1. Introduction

The state selective photodissociation of molecules or molecular ions has received a significant amount of interest in the last decade. Among the properties one is interested in are the state selective decay rates and the dissociation energies. With multicolor laser experiments becoming more and more routinely available these experiments can now be expected to provide us with a wealth of state selective information. Throughout this work the term state selective is meant to imply complete control of the rotational and if applicable the orbital and spin angular momentum of the dissociating molecules. A very intriguing example is the state selective photodissociation of hydrogen peroxide (HOOH) which has been reported recently by Kuhn et al.[1] Other systems where the dissociation has been investigated with contributions from two rotational states are the nitrogen oxide (NO_2)[2] and the methoxy radical (CH_3O).[3] An example of a molecular ion for which the fragmentation kinetics has been investigated by means of photodissociation with high rotational resolution is the benzene ion.[4] Rotationally resolved photodissociation spectra have recently also been reported for the $MgAr^+$ ion,[5] the N_3^+ ion,[6] and the OCS^+ ion.[7]

In this work we will present our first experiments which prove that the photodissociation of a small molecular ion is feasible with complete control of the rotational, orbital, and spin angular momentum as well as the parity. As an example we have chosen hydrogen bromide (HBr), for which a considerable amount of spectroscopic information is available from the literature. The formation of hydrogen bromide ions (HBr^+) via various 2+1 resonance-enhanced multiphoton ionization (REMPI) transitions has been investigated by Callaghan and Gordon.[8] Most relevant to our work are the REMPI spectra resonantly enhanced via either the F $^1\Delta_2$ or the f $^3\Delta_2$ state. By analyzing the laser-induced fluorescence spectrum (LIF) obtained after forming HBr^+ ions in a 2+1 REMPI process via the F $^1\Delta_2$-$(v'''=0)$ Rydberg state Xie and Zare[9] have shown that this ionization pathway leads to ions in only one vibrational state of one spin−orbit component of the ion ground state, i.e., the $^2\Pi_{1/2}(v''=0)$ state. It was further mentioned that resonance enhancement via the f $^3\Delta_2$ state leads selectively to ions in the vibrational ground state of the other spin−orbit component, i.e., the $^2\Pi_{3/2}(v''=0)$ state. More interestingly this process leads predominantly to ions in four different rotational states. This result was confirmed by Wales et al.[10] by recording the photoelectron spectrum of HBr after ionization via these 2+1 REMPI transitions. Thus, the 2+1 REMPI spectrum of HBr provides access to molecular ions in a selected vibronic state with a rather small rotational-state distribution, an almost ideal prerequisite for the study of state selective photodissociation.

The first excited electronic state of HBr^+ is the $^2\Sigma^+$ state which predissociates above a certain threshold. This predissociation is, for example, evident from a significant line broadening in the He I photoelectron spectrum[11] and also in the one-photon ZEKE photoelectron spectrum.[12] Several rotationally resolved fluorescence studies of the $^2\Sigma^+(v'=0, 1) \rightarrow {}^2\Pi_i(i=1/2, 3/2; v''=0, 1)$ transitions have been reported in the literature.[13−15] The $^2\Sigma^+(v'=2)$ state has not been observed by fluorescence, most likely because of predissociation. The same applies for the even higher vibrational states in the $^2\Sigma^+$. From electronic structure calculations it was concluded that the predissociation is made possible by coupling of the $^2\Sigma^+$ to a $^4\Sigma^-$, a $^2\Sigma^-$, and a $^4\Pi$ state.[16] In this work we describe the state selective photodissociation of HBr^+ ions via the $^2\Sigma^+(v'=1, 2, 3, 4) \leftarrow {}^2\Pi_i(i=1/2, 3/2; v''=0)$ transitions.

The experiment performed in this work consists of two steps: (i) the formation of ions and (ii) the photodissociation of these ions. Thus we conduct an optical-optical double-resonance experiment, where the first step serves as a preselection of rotational eigenstates and the second step allows a state selective photodissociation. A total of four different electronic states are involved in each experiment described in this work, i.e., the ground state of neutral HBr (X $^1\Sigma^+$), an intermediate Rydberg state (F $^1\Delta_2$ or f $^3\Delta_2$), the ion ground state (X $^2\Pi_{1/2}$ or X $^2\Pi_{3/2}$), and the first excited electronic state of HBr^+ (A $^2\Sigma^+$). The excitation scheme and the relevant potential

* weitzel@chemie.fu-berlin.de.

S1089-5639(97)03238-6 CCC: $15.00
Published on Web 02/20/1998

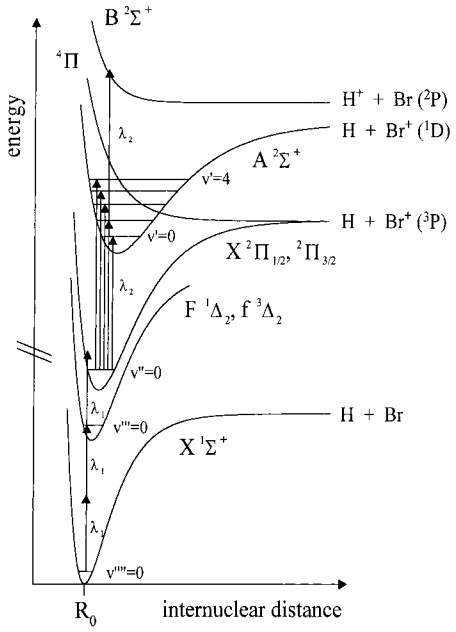

Figure 1. Schematic diagram of the excitation steps in the current experiment and the relevant potential energy curves, based on information from the literature as discussed in the text. Note that the $^4\Pi$ state is not the only repulsive state relevant for the predissociation of the HBr^+ ion.

energy curves of HBr are schematically illustrated in Figure 1. To avoid confusion of quantum numbers associated with the different electronic states, we add successive primes in going from the highest to the lowest state involved, e.g. v', v'', v''', and v'''' for the vibrational states. Only one schematic curve is drawn for the two Rydberg states of neutral HBr as well as the two spin−orbit components of the ion ground state in Figure 1. In one experiment we also describe the formation of H^+ ions via 1+1 two-photon dissociation of the ion. This process presumably includes the repulsive B $^2\Sigma^+$ state, which is also shown in Figure 1.

2. Experimental Technique

All experiments have been performed in a linear time-of-flight mass spectrometer. The sample is introduced into the ion source of the spectrometer as a skimmed molecular beam formed by expanding pure HBr at a stagnation pressure of a few mbar through a 200 μm nozzle. These very mild expansion conditions result in a reduction of the effective translational temperature of the molecules but basically no rotational cooling. The former is an advantage with regard to the mass resolution of the TOF spectrometer as well as to the effective Doppler width relevant for the laser excitation. The axis of the TOF spectrometer and that of the molecular beam and two laser beams are perpendicular with respect to each other and cross in the center of the ion source. In the first step of the experiment HBr^+ ions are formed from neutral molecules by resonance-enhanced multiphoton ionization. In the second step these HBr^+ ions are excited by a second laser to the $^2\Sigma^+$ state, which can predissociate above a certain energetic threshold to form Br^+ ions. The ions are analyzed in the TOF mass spectrometer. The optical resolution of the ionizing laser was 0.15 cm^{-1}; that of the dissociating laser, 0.08 cm^{-1}. Wavelength calibration was performed by comparison to the optogalvanic spectrum of neon. All excitation energies listed in this work are vacuum wavenumbers. Typical laser pulse energies and focusing conditions were $E = 1$ mJ, $f = 100$ mm for the first laser and

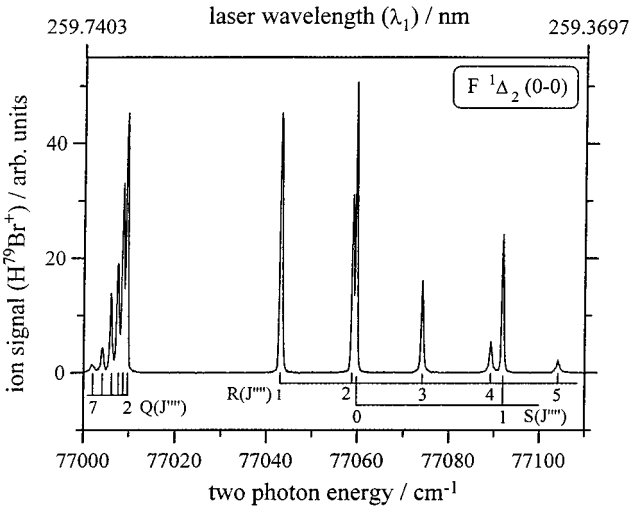

Figure 2. 2+1 REMPI spectrum of HBr via the F $^1\Delta_2(v'''=0) \leftarrow {}^1\Sigma^+$-($v''''=0$) transition. Only the Q- and part of the R- and S-branch are shown.

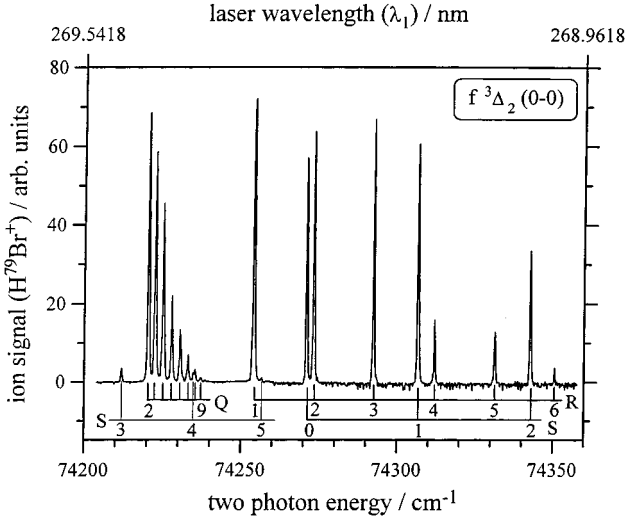

Figure 3. 2+1 REMPI spectrum of HBr via the f $^3\Delta_2(v'''=0) \leftarrow {}^1\Sigma^+$-($v''''=0$) transition. Only the Q- and part of the R- and S-branch are shown. The peaks marked as S(3) to S(5) (lower left corner) belong to another REMPI transition via the f $^3\Delta_3$ Rydberg state.[8]

$E = 200$ μJ, $f = 440$ mm for the second. Some line width measurements were performed without focusing the second laser employing a pulse energy of about 40 μJ. For the two-color experiment the delay between the two lasers was about 100 ns. HBr has been purchased from Messer-Griesheim (purity 99.8%).

3. Results and Discussion

3.1. Preparation of HBr^+ via the 2+1 REMPI Process. In the first section of the results we will describe the first step of the experiment, i.e., the formation of HBr^+ ions in various rotational states of either the $^2\Pi_{1/2}(v''=0)$ state or the $^2\Pi_{3/2}(v''=0)$ state. Here HBr molecules are ionized by a 2+1 resonance-enhanced multiphoton ionization (REMPI), where two photons are resonant with the F $^1\Delta_2(v'''=0)$ or the f $^3\Delta_2(v'''=0)$ Rydberg state. The 2+1 REMPI spectra are obtained by collecting all parent ions as a function of the laser wavelength. The sample investigated in this work actually contains a natural mixture of the two bromine isotopes: ^{79}Br (50.69%) and ^{81}Br (49.31%).[17] Figure 2 and Figure 3 show the 2+1 REMPI spectra recorded for the parent ion containing the light bromine isotope ($H^{79}Br^+$) with the F $^1\Delta_2(v'''=0)$ and the f $^3\Delta_2(v'''=0)$ respectively

TABLE 1: Expected Changes in the Quantum Numbers of the Total Angular Momentum *J* and Rotational Angular Momentum *R* for the R(1) Transition of the REMPI Spectrum Obtained via the F $^1\Delta_2$ State

state	*J*, *R*			
$^1\Sigma^+$	$J'''' = R'''' = 1$			
F $^1\Delta_2$	$J''' = 2, R''' = 0$			
$^2\Pi_{1/2}$	$J'' = 0.5$, $R'' = 0$	$J'' = 1.5$, $R'' = 1$	$J'' = 2.5$, $R'' = 2$	$J'' = 3.5$, $R'' = 3$

as the resonant intermediate state. The spectra recorded for the $H^{81}Br^+$ ion are basically identical. Both REMPI spectra are rotationally resolved and show the Q-, and part of the R- and the S-branch. The O- and the P-branch have not been investigated because we are mainly interested in forming ions in high rotational states. Here the designation of rotational branches as, for example, Q, R, and S has the standard meaning of referring to changes in the quantum number of the total angular momentum of $\Delta J = 0$, 1, and 2. We would like to stress that the rotational quantum number will also be denoted *R* throughout this work. The distinction, however, is unambiguous since the latter is always marked by a number of primes characterizing the given electronic state, i.e., *R*′, *R*″, *R*‴, and *R*⁗.

The most obvious difference between the two REMPI spectra of Figure 2 and Figure 3 is observed in the Q-branch, which extends to lower excitation energies in the former and to higher excitation energies in the latter case, reflecting the corresponding change in rotational constants upon excitation of the HBr. Note that the first members of the Q-, R-, and S-branch are Q(2), R(1), and S(0), because the intermediate state is a Δ state. The line positions in both spectra agree to within 0.6 cm^{-1} with the values tabulated by Callaghan and Gordon.[8] A table including the energies of all transitions observed in the two REMPI spectra is available from the authors by e-mail upon request. Our data confirm the spectroscopic parameters of the intermediate Rydberg states reported by Callaghan and Gordon.[8]

As mentioned in the Introduction, the 2+1 REMPI process described above leads to HBr^+ ions almost exclusively in one vibronic state but with a rotational state distribution typically dominated by four different rotational states. The latter is due to the fact that the selection rules for the absorption of the third photon in this 2+1 REMPI process is $|\Delta J| \leq l + 3/2$,[18,19] where *l* is the quantum number of the orbital angular momentum associated with the partial wave character of the outgoing electron. Wales et al.[10] have shown that this final ionization step is dominated by $\Delta J = \pm 1/2$ and $\pm 3/2$ transitions for this 2+1 REMPI process.

An example of the expected changes in angular momentum quantum numbers is given in Table 1 for the R(1) pump transition via the F $^1\Delta_2(v''' = 0)$ state. In this case ions would be formed with $R'' = 0$, 1, 2, 3 and $J'' = 0.5$, 1.5, 2.5, 3.5, respectively. Note, however, that for the R(1) pump transition via the f $^3\Delta_2(v''' = 0)$ state ions are formed in only three different rotational states, i.e., $R'' = 0$, 1, 2 for $J'' = 1.5$, 2.5, 3.5, respectively, since no $J'' = 0.5$ state exists in the $^2\Pi_{3/2}$ ion ground state.

3.2. State Selective Photodissociation of HBr^+ via the $^2\Sigma^+(v'=2) \leftarrow {}^2\Pi_i(i=1/2, 3/2; v''=0)$ Transition. In the second step of the experiment we tune the first laser to one of the rotational transitions in the REMPI spectra (cf. Figure 2 and Figure 3) and scan the second laser across the region of the $^2\Sigma^+(v'=2) \leftarrow {}^2\Pi_i(i=1/2, 3/2; v''=0)$ transitions. In this experiment the optical transitions are identified by detecting the fragment ion $^{79}Br^+$ or $^{81}Br^+$. Thus we measure the absorption spectrum of the ion above its dissociation threshold. These photodissociation spectra (PD spectra) have been recorded for a large number of R-, S-, and Q-lines of both REMPI spectra. As an example the PD spectra of the $H^{79}Br^+$ ion obtained via the first R pump lines with the F $^1\Delta_2(v''' = 0)$ and the f $^3\Delta_2(v''' = 0)$ intermediate state are displayed in Figure 4 and Figure 5, respectively. Both spectra exhibit resolved fine structure corresponding to resonance states interacting with the dissociation continuum. At first glance the two spectra do not seem to have much in common.

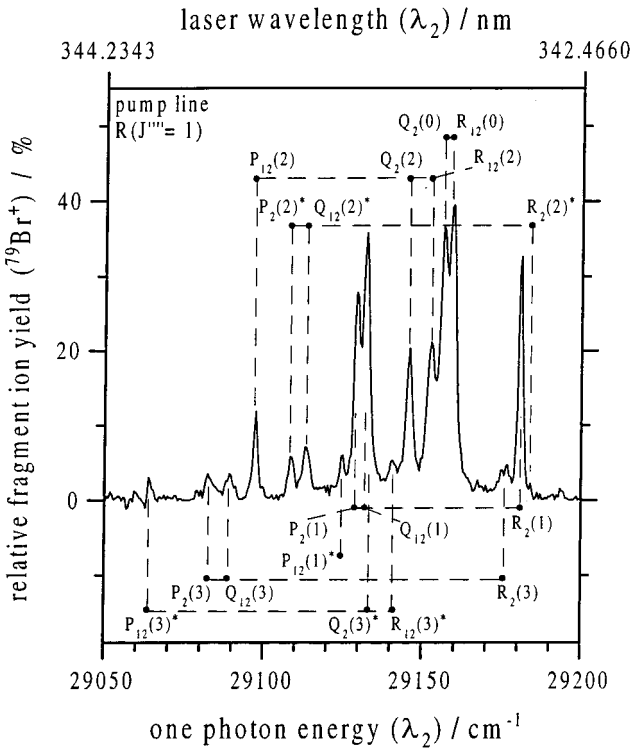

Figure 4. Photodissociation spectrum of HBr^+ ions via the $^2\Sigma^+(v'=2, J', R') \leftarrow {}^2\Pi_{1/2}(v''=0, J'', R'')$ transition. The pump line is R(1) of the REMPI spectrum in Figure 2. All the prominent peaks are assigned according to the scheme in Figure 6. Peaks marked with an asterisk correspond to an initial state with negative parity; those without an asterisk, to positive parity. For further discussion see the text.

To assign these spectra, one needs to recall the angular momentum coupling schemes operative in the two electronic states involved in the photodissociation of the ions. The $^2\Pi$ ground state of the HBr^+ ion is split into two components, $^2\Pi_{1/2}$ and $^2\Pi_{3/2}$, by spin−orbit coupling. The spin−orbit coupling constant is $A = -2653$ cm^{-1},[20] with the $^2\Pi_{3/2}$ component being energetically lower (inverted spin−orbit splitting). Here we will first discuss the photodissociation experiments starting from the $^2\Pi_{1/2}$ state of the ion. We will return to the $^2\Pi_{3/2}$ state afterward. Since the spin−orbit coupling is much stronger than the spin−rotation coupling, the $^2\Pi_{1/2}$ state has often been described as Hund's case a,[10,23] and we will adopt this notation throughout this work. However, it has been pointed out that Hund's case c would in principle be more appropriate.[9] Each angular momentum state (with $R'' = J'' - 1/2$) is split into two components by orbit−rotation coupling (often referred to as Λ-doubling). The two components of each Λ-doublet differ in parity with an alternating parity sequence (+ −, − +, ...) for successive rotational states (with increasing *R*″). The first excited electronic state of HBr^+ ($^2\Sigma^+$) belongs to Hund's case b. This is operative for states without orbital angular momentum and with spin−rotation coupling. Because of spin−rotation coupling, each rotational state (*R*′) is split into two components

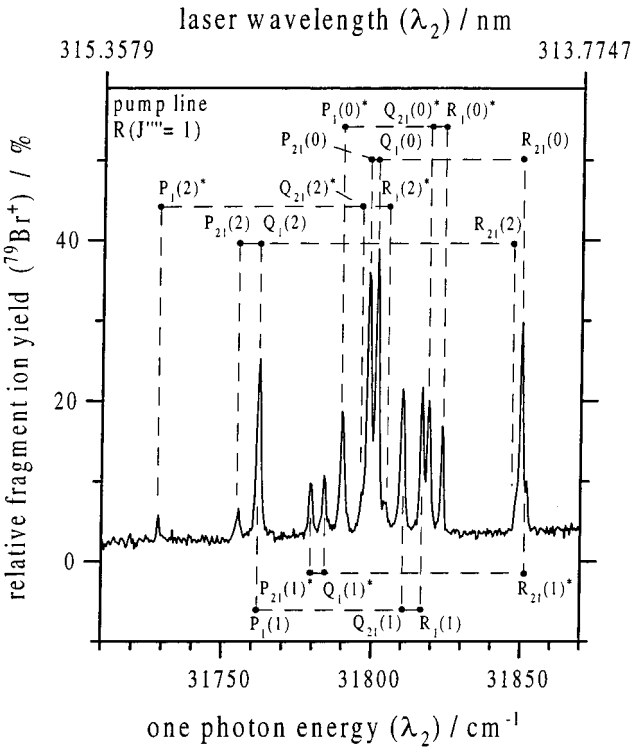

Figure 5. Photodissociation spectra of HBr^+ ions via the $^2\Sigma^+(v'=2, J', R') \leftarrow {}^2\Pi_{3/2}(v''=0, J'', R'')$ transition. The pump line is R(1) of the REMPI spectrum in Figure 3. All the prominent peaks have been assigned as discussed in the text. Peaks marked with an asterisk correspond to an initial state with negative parity; those without an asterisk, to positive parity. For further discussion see the text.

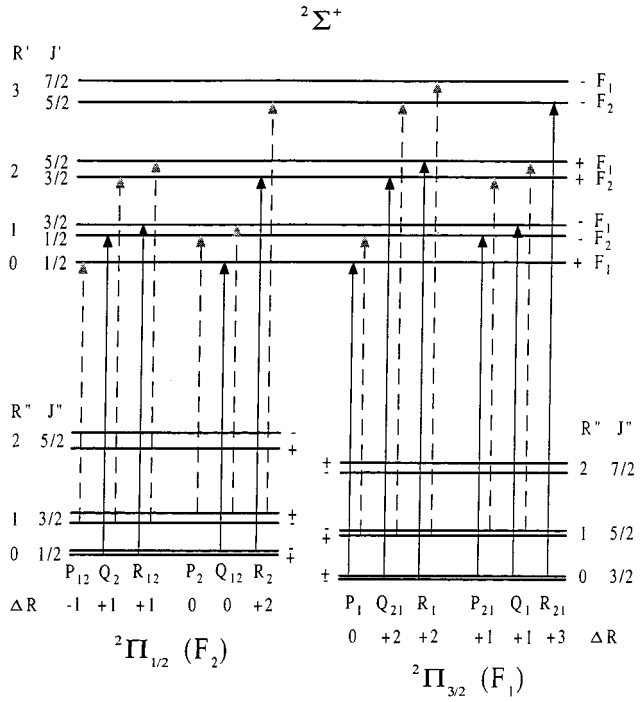

Figure 6. Schematic energy diagram for the $^2\Sigma^+(J', R') \leftarrow {}^2\Pi_{1/2}(J'', R'')$ and the $^2\Sigma^+(J', R') \leftarrow {}^2\Pi_{3/2}(J'', R'')$ transition. Adapted to the current problem from ref 20. Transitions starting from states with identical R'' are marked by identical type of lines.

leading to the respective total angular momentum ($J' = R' \pm 1/2$). Since the parity of a $^2\Sigma^+$ state is determined by the parity of its rotational wave function (which is positive for $R' =$ even, and negative for $R' =$ odd), the two J' components resulting from the spin−rotation coupling have the same parity. The coupling scheme discussed above is illustrated in Figure 6. In the current experiment we tune the second laser into resonance with the allowed transitions, also shown in Figure 6. The important point is that there is a total of six allowed optical transitions for each rotational state in the $^2\Pi_{1/2}$ (except for the $R'' = 0$ state, for which there are only four allowed transitions). The nomenclature used in this work to characterize the observed transitions is $P_{12}(\Delta J = -1, \Delta R = -1)$, $Q_2(\Delta J = 0, \Delta R = +1)$, $R_{12}(\Delta J = +1, \Delta R = +1)$, $P_2(\Delta J = -1, \Delta R = 0)$, $Q_{12}(\Delta J = 0, \Delta R = 0)$, and $R_2(\Delta J = +1, \Delta R = +2)$. Here the capital letter denotes the change in J. The subscript "12" denotes a transition $F_1 \leftarrow F_2$, while the subscript "2" denotes a transition $F_2 \leftarrow F_2$. All eigenstates of the $^2\Pi_{1/2}$ state belong to F_2. In the $^2\Sigma^+$ state those eigenstates with $J' = R' + 1/2$ belong to F_1 and those with $J' = R' - 1/2$ to F_2.

In the $^2\Pi_{3/2}$ state the same coupling scheme applies as in the $^2\Pi_{1/2}$ state. However, here the parity sequence in the Λ-doublets for successive rotational states is just opposite of that in the $^2\Pi_{1/2}$ state, i.e., (− +, + −, ...). The quantum numbers of the rotational and the total angular momentum are related by $R'' = J'' - 3/2$. All eigenstates of the $^2\Pi_{3/2}$ belong to F_1, and thus the following optical transitions are allowed: $P_1(\Delta J = -1, \Delta R = 0)$, $Q_{21}(\Delta J = 0, \Delta R = +2)$, $R_1(\Delta J = +1, \Delta R = +2)$, $P_{21}(\Delta J = -1, \Delta R = +1)$, $Q_1(\Delta J = 0, \Delta R = +1)$, and $R_{21}(\Delta J = +1, \Delta R = +3)$. The allowed transitions starting from this $^2\Pi_{3/2}$ state are also included in Figure 6.

Every single line in the dissociation spectra shown in Figures 4 and 5 has been assigned to an optical transition of the kind $^2\Sigma^+(v'=2, J', R') \leftarrow {}^2\Pi_i(i=1/2, 3/2; v''=0, J'', R'')$ according to the scheme discussed above. For example, the designation $P_{12}(2)$ stands for a transition starting from a state with the rotational quantum number $R'' = 2$ in the ion ground state. Thus each line corresponds to the dissociation of HBr^+ ions with precisely defined rotational, orbital, and spin angular momentum. We would like to draw attention to some general features of these PD spectra and their assignment. The PD spectrum in Figure 4 contains peaks starting from four different rotational states in the $^2\Pi_{1/2}$ state. The spectrum in Figure 5 contains contributions from only three different rotational states in the $^2\Pi_{3/2}$ state. As mentioned earlier, this difference is due to the fact that there is no state with $J = 1/2$ in the $^2\Pi_{3/2}$ state. In the assignment of the peaks in Figure 4 and Figure 5 those transitions starting from the same rotational state R'' with the same parity are grouped together. In both PD spectra (Figure 4 and Figure 5) all transitions starting from a state with negative parity are marked by an asterisk, but those starting from positive parity are not. Clearly the peaks without an asterisk dominate in Figure 4. This dominance is much less pronounced in Figure 5. For both R(1) pump lines the REMPI process of ion formation starts from the $J'''' = R'''' = 1$ state, i.e., a state with negative parity. Since the parity is not allowed to change in the two-photon resonant part of the REMPI process, the observation of predominantly ions with positive parity in the $^2\Pi_i$ state implies that the parity of the ion does change in the final ionization step. Similar observations have been reported and analyzed for this REMPI process before.[9,10,21] The dominance of ions being formed in one parity state indicates that the photoelectron emitted in the final ionization step has predominantly s and/or d partial wave character. However, contributions from p and f partial waves cannot be neglected. This has been explained by deviations from atomic-like dynamics in the photoelectron emission due to the angular momentum composition of the intermediate Rydberg states.[21] In this work we will concentrate on the spectroscopic analysis of the PD

TABLE 2: Experimentally Determined Transition Energies in cm^{-1} from the Photodissociation Spectra of $H^{79}Br^+$ Ions via the $^2\Sigma^+(v'=2, J', R') \leftarrow {}^2\Pi_{1/2}(v''=0, J'', R'')$ Transition. Most Entries Have Been Determined via More than One Pump Line in the REMPI Spectrum and Do Represent an Average Value in That Case

optical transition:		P_{12}	Q_2	R_{12}	P_2	Q_{12}	R_2
ΔR:		−1	+1	+1	0	0	+2
R''	J''						
0	1/2		29 156.4	29 159.1		29 145.5	29 174.6
1	3/2	29 124.7	153.8	158.6	29 129.3	132.0	180.4
2	5/2	097.2	145.6	152.2	108.6	113.2	180.9
3	7/2	064.2	132.5	140.7	082.5	089.0	176.2
4	9/2	026.0	113.5	123.6	051.3	059.4	166.0
5	11/2	28 983.1	089.7	101.7	014.8	025.5	150.2
6	13/2	934.9	059.8	073.7	28 972.8	28 983.9	129.0
7	15/2	880.8	025.2	040.4	925.6	939.2	102.5
8	17/2		28 984.0	002.0			

TABLE 3: Experimentally Determined Transition Energies in cm^{-1} from the Photodissociation Spectra of $H^{79}Br^+$ Ions via the $^2\Sigma^+(v'=2, J', R') \leftarrow {}^2\Pi_{3/2}(v''=0, J'', R'')$ Transition. Most Entries in This Table Have Been Determined via More than One Pump Line in the REMPI Spectrum and Do Represent an Average Value in that Case

optical transition:		P_1	Q_{21}	R_1	P_{21}	Q_1	R_{21}
ΔR:		0	+2	+2	+1	+1	+3
R''	J''						
	1/2						
0	3/2	31 789.8	31 819.0	31 823.6	31 798.9	31 801.6	31 849.9
1	5/2	761.8	810.3	816.7	779.2	783.9	851.8
2	7/2	728.5	796.2	804.3	755.0	761.9	848.2
3	9/2	689.8	777.2	787.2	725.1	733.2	839.4
4	11/2	648.0	752.8	764.2	689.8	700.0	825.1
5	13/2	597.4	722.7	736.4	649.7	662.0	805.7
6	15/2	543.0	688.4	702.9	604.1	618.2	780.5
7	17/2	483.9	646.9	663.8	553.2	568.3	750.6
8	19/2		601.0	619.6	497.3	513.5	714.1
9	21/2		549.0	569.8			672.2
10	23/2		493.0	514.0			625.5
11	25/2						572.0

spectra and some specific details regarding the predissociation process. The analysis of the different parity transitions in the REMPI process will be discussed elsewhere. The optical transition energies of all peaks observed in our PD spectra for the $H^{79}Br^+$ ions including the spectroscopic assignment are listed in Table 2 and Table 3. The corresponding data for the $H^{81}Br^+$ ions are slightly shifted (on the average by less than 0.5 cm^{-1}). These data can be obtained from the authors upon request. From the analysis of the optical transition energies described above information can be derived regarding the rotational constants in the corresponding electronic states and also the Λ-doubling in the $^2\Pi_{1/2}$ state and the spin-rotation coupling in the $^2\Sigma^+$ state.

The Λ-doubling is found to increase linearly with increasing rotational angular momentum for the $^2\Pi_{1/2}$ state. The observed transition energies have been fitted to eq 1, where p is the first Λ-doubling constant and b is the ordinate segment.

$$\Lambda(R'') = p(R'' + 1) + b \qquad (1)$$

The analysis of our data according to eq 1 yields $p = 2.01 \pm 0.06$ cm^{-1} and $b = 0.4 \pm 0.15$ cm^{-1}. Within the error limits this value for p is in agreement with numbers reported by Norling[13] and Barrow et al.,[14] who applied the same formula. It is also compatible with values reported by Lubic et al.[22] and Chanda et al.[23] In the $^2\Pi_{3/2}$ state the Λ-doubling is too small to be measured accurately in our experiment (<0.1 cm^{-1}) for the given rotational states. Therefore we did not attempt to derive a value for the second Λ-doubling constant q.

The spin−rotation coupling can be directly read from the PD spectra. Both spectra shown in Figure 4 and Figure 5 exhibit several prominent doublets, whose splitting increases with increasing R'' and whose center shifts to lower excitation energy. In the spectrum recorded via the $^2\Pi_{1/2}$ state (Figure 4) these doublets arise from the Q_2, R_{12} and the P_2, Q_{12} transitions, and in the spectrum recorded via the $^2\Pi_{3/2}$ state (Figure 5) they arise from the Q_{21}, R_1 and the P_{21}, Q_1 transitions. The spin−rotation coupling is commonly described by eq 2, where γ is the spin−rotation coupling constant.

$$2\Delta\tilde{\nu}_\gamma(R') = \gamma(R' + 1/2) \qquad (2)$$

TABLE 4: Comparison of the Spin−Rotation Coupling Constant γ in the $^2\Sigma^+(v'=2)$ State from This Work with Values from the Literature

	this work	ref 13	ref 14
$\gamma(v'=0)/cm^{-1}$		2.08	2.10
$\gamma(v'=1)/cm^{-1}$		2.01	2.03
$\gamma(v'=2)/cm^{-1}$	1.81 ± 0.09		

For the extraction of the spin−rotation coupling constant the two sets of PD spectra recorded via the different spin−orbit components of the $^2\Pi_i$ state were analyzed separately. From the analysis (of a total of 21 transitions in the case of the $^2\Pi_{1/2}$ state) we arrive at $\gamma = 1.81 \pm 0.16$ cm^{-1} via the $^2\Pi_{1/2}$ state and $\gamma = 1.81 \pm 0.09$ cm^{-1} via the $^2\Pi_{3/2}$ state. This proves that the information derived for the $^2\Sigma^+$ state is independent of the spin−orbit component of the ion ground state chosen for pumping the $^2\Sigma^+$ state. This spin−rotation coupling $\gamma_{v'=2}$ has been determined for the first time. The comparison with data available for the lower vibrational states of the $^2\Sigma^+$ state (see Table 4) reveals that γ decreases with increasing vibrational excitation in the $^2\Sigma^+$ state.

With the information regarding the spin−rotation coupling in the $^2\Sigma^+$ state and the orbit−rotation coupling in $^2\Pi_i$ electronic

TABLE 5: Comparison of the Rotational Constant B' in the $^2\Sigma^+$ State from This Work with Values from the Literature

	this work	ref 13	ref 14
$B'(v'=0)/cm^{-1}$		5.85	5.846
$B'(v'=1)/cm^{-1}$		5.60	5.598
$B'(v'=2)/cm^{-1}$	5.22 ± 0.06		

states the rotational constants B can also be determined. The analysis yields $B'' = 7.91 \pm 0.12$ cm^{-1} for the $^2\Pi_{1/2}(v'=0)$ state and $B'' = 7.88 \pm 0.06$ cm^{-1} for the $^2\Pi_{3/2}(v'=0)$ state. Within the error limits the same value is observed for the two spin−orbit components of the $^2\Pi_i$ state. This is in line with information available from the literature.[13,14,22,23] The rotational constant of the $^2\Sigma^+(v'=2)$ state has been determined for the first time. We derive a value of $B' = 5.24 \pm 0.04$ cm^{-1} via the $^2\Pi_{1/2}$ state and $B' = 5.20 \pm 0.06$ cm^{-1} via the $^2\Pi_{3/2}$ state. This again proves that the information obtained regarding the $^2\Sigma^+$ state is independent of the spin−orbit component of the $^2\Pi_i$ state used in the experiment. Centrifugal distortion constants have not been derived from our data. In Table 5 the rotational constant B' ($v'=2$) is compared to data reported in the literature for lower vibrational states in the $^2\Sigma^+$. Evidently the rotational constant decreases monotonically with increasing vibrational excitation.

3.3. *J* Dependence of the Dissociation Threshold. In the previous section the state selective photodissociation of the HBr^+ ions in the $^2\Sigma^+(v'=2)$ state was described. In that experiment the lowest 15 rotational eigenstates of the $^2\Sigma^+(v'=2)$ state have been observed in the PD spectra. This implies that all angular momentum eigenstates in this state decay by predissociation. One may now ask the question if the $^2\Sigma^+(v'=1)$ state can also be observed in photodissociation and how many rotational quanta are necessary to reach the dissociation threshold. In general the search for such a dissociation threshold is difficult because one looks for the absence of a fragment ion signal on a spectrally narrow transition whose position is not precisely known in the first place. In this situation we took advantage of the fact that the one-photon dissociation leading to Br^+ ions can compete with the two-photon dissociation where the first photon is resonant with the $^2\Sigma^+(v'=1) \leftarrow {}^2\Pi_i(i=1/2, 3/2; v''=0)$ transition. The latter process leads to the formation of H^+ ions most likely via direct dissociation of a repulsive excited state. From the energetic point of view the relevant state could be the B $^2\Sigma^+$ state.[16] The relative yield of Br^+ and H^+ ions depends on the relative magnitude of the rate constant for predissociation and the absorption probability for another photon in the $^2\Sigma^+(v'=1)$ state. Under our experimental conditions this two-photon dissociation is only observed via the $^2\Sigma^+(v'=1)$ state. It is not observed for any of the higher vibrational states $^2\Sigma^+(v' \geq 2)$, suggesting that most of the molecular ions predissociate before they can absorb another photon.

The important advantage of this experiment is that it enables us to record the (rotationally resolved) absorption spectrum of the $^2\Sigma^+(v'=1) \leftarrow {}^2\Pi_i(i=1/2, 3/2; v''=0)$ transition even below the energetic limit for one-photon dissociation. These two-photon dissociation spectra can be assigned in analogy with the $^2\Sigma^+(v'=2) \leftarrow {}^2\Pi_i(i=1/2, 3/2; v''=0)$ transitions. We then only have to search which transitions are observed in the Br^+ ion yield spectrum, i.e., the one-photon dissociation spectrum, and which are missing. The result of this search is illustrated in Figure 7, where the H^+ ion spectrum (lower trace) and the Br^+ ion spectrum (upper trace) are compared. As mentioned above, each rotational state in the $^2\Sigma^+$ is split into two components by spin−rotation coupling ($J' = R' \pm 1/2$). The spectra in Figure 7 show that the $J' = 12.5$, $R' = 12$ state leads to the formation

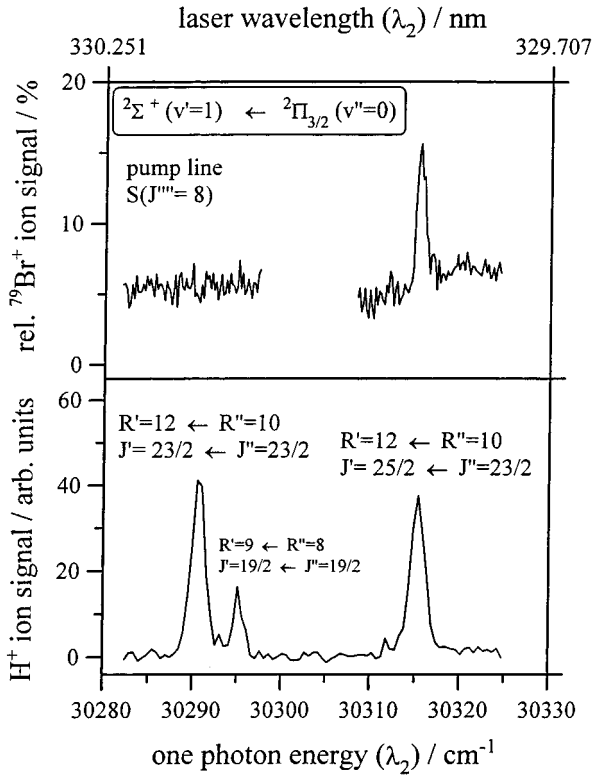

Figure 7. Photodissociation spectra of HBr^+ ions via the $^2\Sigma^+(v'=1) \leftarrow {}^2\Pi_{3/2}(v''=0)$ transition. Lower curve: H^+ ion yield (two-photon dissociation). Upper trace: Br^+ ion yield (one photon dissociation). Note that the $^2\Sigma^+(v'=1, J'=11.5, R'=12)$ state is observed in the H^+ spectrum but not in the $^{79}Br^+$ spectrum.

of Br^+ ions whereas the $J' = 11.5$, $R' = 12$ state does not. Since all higher rotational states we searched for are also observed in the Br^+ spectrum and all lower states are missing, we conclude that there is an unambiguous energetic limit for the predissociation in the $^2\Sigma^+(v'=1)$ state. We do not see any indication that this experimentally determined threshold might be affected by a kinetic shift (cf. also next section). The energetic threshold derived in this work is in agreement with a value reported by Haugh and Bayes.[15] In that work the threshold energy was derived from measuring the decrease in the fluorescence intensity observed from a hot discharge source. Certainly the two approaches of detecting the fragment ion and the fluorescence of the molecular ion are complementary in this case. With respect to future investigations of the role of rotation in the dissociation of nonlinear polyatomic ions the photodissociation spectroscopy employed in this work seems to be more specific and more universal. In any case the current work demonstrates that it is possible to determine dissociation energies with rotational resolution. Here we conclude that the first predissociating rotational state within the $v' = 1$ state has an energy of 2203.6 cm^{-1} referenced to the rotationless state of the $^2\Sigma^+(v'=0)$ state. The rotational ground state of the $^2\Sigma^+(v'=2)$ state, which is also observed in the PD spectra, occurs at an energy of 2575.7 cm^{-1} above the $^2\Sigma^+(v'=0)$ state.

3.4. Lifetime for Predissociation of HBr^+. Every single peak in the PD spectra shown in Figures 4 and 5 corresponds to an eigenstate of the $^2\Sigma^+(v'=2)$ state interacting with the dissociation continuum. The width of each peak is correlated to the lifetime of that resonance state. However, other possible contributions to the experimental line width have to be taken into account. Under the conditions employed in recording the PD spectra shown in Figures 4−7 typical line widths were on the order of 4 cm^{-1}. This value turned out to be dominated by

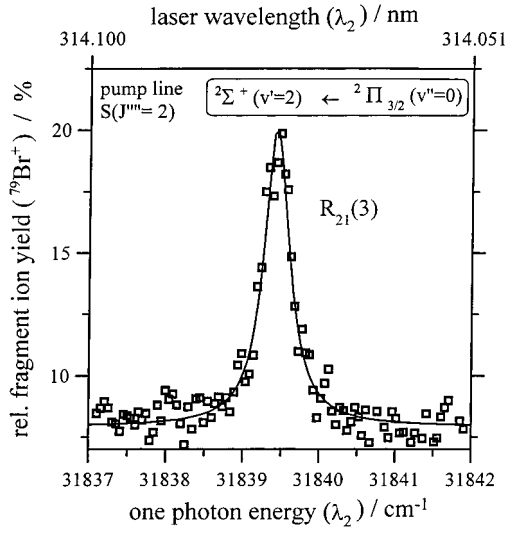

Figure 8. Photodissociation spectrum of HBr^+ ions via the $^2\Sigma^+(v'=2, J'=5.5, R'=6) \leftarrow {}^2\Pi_{3/2}(v''=0, J''=4.5, R''=3)$ transition: (□) experimental data; (—) Lorentzian function with fwhm = 0.4 cm^{-1}.

power broadening effects. To investigate the line width, some resonance lines have been remeasured employing no focusing of the second laser (diameter ca. 2 mm) and a pulse energy of about 40 μJ. This is the lowest pulse energy at which we were able to measure PD spectra with a reasonable signal/noise ratio. Under these conditions the line width observed in the PD spectra was 0.35−0.4 cm^{-1} for rotational quantum numbers in the $^2\Sigma^+$-($v'=2$) state of $R' = 0$, 2, 4, 6, 8, and 10. A typical spectrum is shown in Figure 8. There the experimental data have been simulated by a Lorentzian function with a full width at half-maximum (fwhm) of 0.4 cm^{-1}. This width (Γ_{tot}) does not directly correspond to the natural lifetime of that resonance state. To estimate this natural line width (Γ_τ), we have employed

$$\Gamma_{tot} = \sqrt{\Gamma_\tau^{\,2} + \Gamma_{dop}^{\,2} + \Gamma_{las}^{\,2} + \Gamma_I^{\,2}} \qquad (3)$$

where Γ_{dop}, Γ_{las}, and Γ_I are the contributions of the Doppler effect (ca. 0.012 cm^{-1}), the optical resolution of the laser (0.08 cm^{-1}), and the nuclear spin−electronic angular momentum coupling (up to 0.2 cm^{-1} [23]), respectively. Taking these contributions into account, we arrive at a natural line width of $\Gamma_\tau = 0.34$ cm^{-1}, corresponding to a lifetime of the $^2\Sigma^+(v'=2)$ state of $\tau_{v'=2} = 16$ ps. A value of $\Gamma_{tot} = 0.35$ cm^{-1} would lead to $\tau_{v'=2} = 19$ ps. Since we cannot prove unambiguously that the experimental line width under these conditions does not contain any saturation broadening, we consider this number to be a lower limit to the true lifetime. As mentioned above, we did not observe a J or R dependence of Γ_{tot}. The PD spectra corresponding to the predissociation of HBr^+ ions in the $^2\Sigma^+$-($v'=1$) state recorded in the search for the J dependence of the dissociation threshold also showed a fwhm of 0.35−0.4 cm^{-1}. In analogy with the $v' = 2$ state we again conclude a lower limit of the predissociation lifetime of $\tau_{v'=1} = 16$ ps. Although we give lower limits only to the lifetimes in the $v' = 2$ and $v' = 1$ state, we should point out that the lifetime of the $v' = 1$ state is probably significantly larger than that of the $v' = 2$ state. This is concluded from the fact that competition with two-photon dissociation is observed in the $v' = 1$ but not in the $v' = 2$ state. On the other hand the lifetime of the $v' = 1$ state cannot be longer than 200 ns. Otherwise we would expect to see an indication of metastable fragmentation in the time-of-flight spectra. Note that this discussion of the lifetime of the $v' = 1$ state applies only to the rotational eigenstates above the threshold for predissociation.

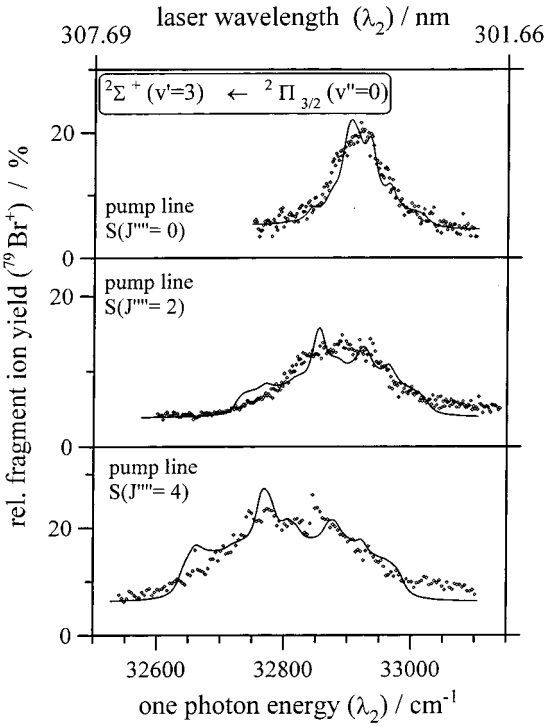

Figure 9. Photodissociation spectra of HBr^+ ions via the $^2\Sigma^+(v'=3) \leftarrow {}^2\Pi_{3/2}(v''=0)$ transition; pump lines S(0), S(2), and S(4): (◇) experimental data; (—) simulation using Lorentzian functions with fwhm = 40 cm^{-1}.

We have also investigated the photodissociation of HBr^+ ions via the next higher vibrational states, i.e., the $^2\Sigma^+(v'=3)$ and $^2\Sigma^+(v'=4)$ states. Three PD spectra of the $^2\Sigma^+(v'=3)$ state recorded on pump lines S(0), S(2), and S(4) of the REMPI spectrum shown in Figure 3, i.e., with the $^2\Pi_{3/2}$ as the intermediate state, are shown in Figure 9. Evidently these PD spectra do not exhibit rotational structure but are rather broad. In the analysis of the line shape one must take into account that more than one rotational state contributes to the spectra. Here we have taken the corresponding PD spectra recorded on the $^2\Sigma^+(v'=2) \leftarrow {}^2\Pi_{3/2}(v''=0)$ transition and convoluted them with a Lorentzian function. The resulting line profiles are also shown in Figure 9. Extracting lifetime information from this simulation implies two assumptions. First we assume that the rotational constant in the $^2\Sigma^+(v'=3)$ state is similar to that in the $^2\Sigma^+(v'=2)$ state. This seems justified since the rotational constants decrease only slightly from $B'(v'=0) = 5.85$ cm^{-1},[13] over $B'(v'=1) = 5.60$ cm^{-1},[13] to $B'(v'=2) = 5.22$ cm^{-1} (this work). Second, using only one Lorentzian function in the simulations implies the assumption that the line width broadening is independent of the rotational state. The analysis of the line shapes in Figure 9 yielded the best fits for Lorentzian functions with fwhm = 40 cm^{-1} for all spectra. The by far dominating contribution to this line width broadening stems from the decrease in the lifetime compared to the $^2\Sigma^+(v'=2)$ state. Here we derive a lifetime of $\tau_{v'=3} = 130 \pm 50$ fs. This number is in agreement with values reported previously.[11,12,16] Within the error limits we do not observe a J dependence of the lifetime. The PD spectra recorded with the $^2\Sigma^+(v'=4)$ as the predissociating state exhibit an even broader line width. These spectra have been simulated by a simple Lorentzian function with $\Gamma_{tot} = 800$ cm^{-1}. This value translates to a lifetime of $\tau_{v'=4} = 7 \pm 3$ fs. Slightly larger values have been reported by Baltzer et

TABLE 6: Lifetimes of the Vibrational States $v' = 0$ to $v' = 5$ of the $^2\Sigma^+$ State. Values Derived in This Work in Comparison with Information from Baltzer et al.,[11] Banichevich et al.,[16] Mank et al.,[12] and Möhlmann et al.[24]

	this work		Baltzer	Banichevich	Mank	Möhlmann
v'	k [s^{-1}]	τ_{dis} [fs]	τ_{dis} [fs]	τ_{dis} [fs]	τ_{dis} [fs]	τ_F [μs]
0				stable		4.5 ± 0.4
1	$<6.3 \times 10^{10}$	>16 000		stable		4.0 ± 0.4
2	$<6.3 \times 10^{10}$	>16 000		152 000		
3	7.5×10^{12}	130	130	153	100	
4	1.5×10^{14}	7	10−15	10.6		
5				10.1		

al.[11] and Banichevich et al.[16] There is no indication that any of the experimental line widths depend on the spin−orbit component of the $^2\Pi_i$ state employed in the experiment.

The lifetime information derived in this chapter is summarized in Table 6. This table focuses on the lifetime for predissociation. Included is also the decay lifetime recorded by Möhlmann et al.[24] for the $^2\Sigma^+(v'=0, 1)$ states. That experiment was dominated by ions in relatively low J states, which are known to decay only by fluorescence. The theoretical study of Banichevich et al. did not take into account the molecular rotation. The designation of the $v' = 0$ and 1 states as stable is supposed to read as $\tau > 1$ ns.[16] Since we have shown that eigenstates with $J' \geq 25/2$ and $R' \geq 12$ predissociate in the $^2\Sigma^+(v'=1)$ state, the total decay lifetime must drop at that level. The experimental studies by Baltzer et al. and Hepburn et al.[12] were characterized by a thermal sample and a cold molecular beam sample of HBr, respectively, employing in both cases one-photon excitation up to the dissociation threshold.

4. Summary

The predissociation spectroscopy of HBr^+ ions has been investigated in an optical−optical double-resonance experiment where the molecular ions are formed by a 2+1 REMPI process in the first step and photodissociated via the $^2\Sigma^+(v'=1, 2, 3$ and $4) \leftarrow {}^2\Pi_i(i=1/2, 3/2, v''=0)$ transitions in the second step. The experiments prove that state selective photodissociation with complete resolution of the rotational, orbital, and spin angular momentum as well as the parity of the HBr^+ ions is possible in the $^2\Sigma^+(v'=1, 2)$. The observation of a photodissociation signal for a total of 15 rotational eigenstates ($R' = 0$ to 14) implies that all angular momentum eigenstates within the $^2\Sigma^+(v'=2)$ state predissociate. The rotational constant $B(v'=2)$ and the spin−rotation coupling constant $\gamma(v'=2)$ have been determined for the first time. They pursue a trend known from the literature for the lower vibrational states in the $^2\Sigma^+$.

The high selectivity in the predissociation spectra via the $^2\Sigma^+(v'=2)$ state becomes possible because lifetime broadening is negligible. From the analysis of the line profiles a lower limit for the lifetime of the $v' = 2$ state has been derived with $\tau_{v'=2} = 16$ ps. With increasing vibrational excitation the lifetime of the $^2\Sigma^+$ state is found to decrease significantly. This leads to a line broadening which precludes rotational resolution. Within the error limits the lifetime of the $^2\Sigma^+$ state is not found to vary with the rotational quantum number. In the direct dissociation of a diatomic molecule this would not be expected in the first place, since the rotational energy effects only the effective threshold for dissociation.[25] However, the dissociation of the HBr^+ ions occurs by predissociation, and the lifetime of the predissociating states is dominated by spin−orbit coupling between the $^2\Sigma^+$ state and several excited repulsive states. Here our experiment suggests that this spin−orbit coupling does not significantly depend on the rotational quantum number. It would be interesting to see a theoretical treatment of this dissociation taking the rotational angular momentum into account. For the future it also seems rewarding to apply the current experiment to nonlinear molecular ions particularly with respect to the role of the K rotor.

The optical−optical double-resonance experiment performed in this work has been based on the idea that the REMPI ionization of HBr in the first step provides a preselection for the succeeding state selective dissociation in the second step. However, the experiment may also be viewed from a different point: that is, the state selective dissociation is evidently a very sensitive probe for competing parity transitions in the 2+1 REMPI process. The analysis of the relative yield of ions formed in different parity states by the REMPI process is currently in progress.

Acknowledgment. Support of this work by the Deutsche Forschungsgemeinschaft (We 1330/3) is gratefully acknowledged. We would also like to thank Prof. H. Baumgärtel for support, particularly for making one of the laser systems available to us, and Prof. E. Illenberger for the loan of a SHG unit.

Supporting Information Available: Two tables with transition energies of the two REMPI spectra shown in Figures 2 and 3 and two tables containing the transition energies of the photodissociation spectra for the $H^{81}Br^+$ ion complementary to Tables 2 and 3 (4 pages). Ordering information is given on any current masthead page.

References and Notes

(1) Kuhn, B.; Boyarkin, O. V.; Rizzo, T. R. *Ber. Bunsen-Ges. Phys. Chem.* **1997**, *101*, 339.
(2) Abel, B.; Hamann, H. H.; Lange, N. *Faraday Discuss. Chem. Soc.* **1995**, *102*, 147.
(3) Dertinger, S.; Geers, A.; Kappert, J.; Wiebrecht, J.; Temps, F. *Faraday Discuss. Chem. Soc.* **1995**, *102*, 31.
(4) Kiermeier, A.; Kühlewind, H.; Neusser, H. J.; Schlag, E. W.; Lin, S. H. *J. Chem. Phys.* **1988**, *88*, 6182.
(5) Scurlock, C. T.; Pilgrim, J. S.; Duncan, M. A. *J. Chem. Phys.* **1995**, *103*, 3293.
(6) Friedman, A.; Soliva, A. M.; Nizkorodov, S. A.; Bieske, E. J.; Maier, J. P. *J. Phys. Chem.* **1994**, *98*, 8896.
(7) Weinkauf, R.; Boesl, U. *J. Chem. Phys.* **1994**, *101*, 8482.
(8) Callaghan, R.; Gordon, R. J. *J. Chem. Phys.* **1990**, *93*, 4624.
(9) Xie, J.; Zare, R. N. *Chem. Phys. Lett.* **1989**, *159*, 399.
(10) Wales, N. P.; Buma, W. J.; de Lange, C. A.; Lefebvre-Brion, H.; Wang, K.; McKoy, V. *J. Chem. Phys.* **1996**, *104*, 4911.
(11) Baltzer, P.; Larsson, M.; Karlsson, L.; Lundqvist, M.; Wannberg, B. *Phys. Rev. A* **1994**, *49*, 737.
(12) Mank, A.; Nguyen, T.; Martin, J. D. D.; Hepburn, J. W. *Phys. Rev. A* **1995**, *51*, R1.
(13) Norling, F. *Z. Phys.* **1935**, *95*, 179.
(14) Barrow, R. F.; Count, A. *Proc. Phys. Soc. (London) A* **1953**, *66*, 617.
(15) Haugh, M. J.; Bayes, K. D. *J. Phys. Chem.* **1971**, *75*, 1472.
(16) Banichevich, A.; Klotz, R.; Peyerimhoff, S. D. *Mol. Phys.* **1992**, *75*, 173.
(17) Weast, R. C., Ed.; *Handbook of Chemistry and Physics*; CRC Press: Boca Raton, 1988.
(18) Xie, J.; Zare, R. N. *J. Chem. Phys.* **1990**, *93*, 3033.
(19) Wang, K.; McKoy, V. *J. Chem. Phys.* **1991**, *95*, 4977.
(20) Herzberg, G. *Molecular Spectra and Molecular Structure: I, Spectra of Diatomic Molecules*; van Nostrand Reinhold: New York, 1950.
(21) Wang, K.; McKoy, V. *J. Chem. Phys.* **1991**, *95*, 7872.
(22) Lubic, K. G.; Ray, D.; Hovde, D. C.; Veseth, L.; Saykally, R. J. *J. Mol. Spectrosc.* **1989**, *134*, 21.
(23) Chanda, A.; Ho, W. C.; Dalby, F. W.; Ozier, I. *J. Mol. Spectrosc.* **1995**, *169*, 108.
(24) Möhlmann G. R.; de Heer, F. *J. Chem. Phys.* **1976**, *17*, 147.
(25) Weitzel, K.-M. *Chem. Phys. Lett.* **1991**, *186*, 490, and references therein.